Phytochemistry 117 (2015) 123–134

Contents lists available at ScienceDirect

Phytochemistry

journal homepage: www.elsevier.com/locate/phytochem

Anti-viral and cytotoxic norbisabolane sesquiterpenoid glycosides from *Phyllanthus emblica* and their absolute configurations

Jun-Jiang Lv [a,c,1], Shan Yu [a,b,1], Ying Xin [a,b], Rong-Rong Cheng [a], Hong-Tao Zhu [a], Dong Wang [a], Chong-Ren Yang [a], Min Xu [a,*], Ying-Jun Zhang [a,*]

[a] State Key Laboratory of Phytochemistry & Plant Resources in West China, Kunming Institute of Botany, Chinese Academy of Sciences, Lanhei Road 132#, Kunming 650201, People's Republic of China
[b] University of Chinese Academy of Sciences, Beijing 100049, People's Republic of China
[c] Chemistry and Chemical Engineering College, Chongqing University, Chongqing 400030, People's Republic of China

ARTICLE INFO

Article history:
Received 4 December 2014
Received in revised form 30 May 2015
Accepted 2 June 2015

Keywords:
Yu Gan Zi
Phyllanthus emblica
Euphorbiaceae
ECD calculation
Antiviral
Norbisabolane sesquiterpenoid glycosides
Phyllaemblicins

ABSTRACT

In an effort to identify anti-viral and cytotoxic compounds from *Phyllanthus* spp., 14 highly oxygenated norbisabolane sesquiterpenoids, phyllaemblicins H1–H14, were isolated from the roots of *Phyllanthus emblica* Linn, along with phyllaemblicins B and C and glochicoccinoside D. Their structures were determined on the basis of detailed spectroscopic analysis and chemical methods. Determination of absolute configurations of these compounds was facilitated by theoretical calculations of electronic circular dichroism (ECD) spectra using time-dependent density functional theory (TDDFT) for the aglycone components, and pre-column derivative/chiral HPLC analysis for the monosaccharides. The known glochicoccinoside D displayed potent activity against influenza A virus strain H3N2 and hand, foot and mouth virus EV71, with IC_{50} values of 4.5 ± 0.6 and 2.6 ± 0.7 μg/ml, respectively. Phyllaemblicin H1 showed moderate cytotoxicity against human cancer cell lines A-549 and SMMC-7721, with IC_{50} values of 4.7 ± 0.7 and 9.9 ± 1.3 μM, respectively.

1. Introduction

Highly oxygenated bisabolane sesquiterpenoid glycosides are primarily present in the roots of several *Phyllanthus* spp. (Euphorbiaceae). Isolation of phyllanthocin from *Phyllanthus brasiliensis* Muell (Kupchan et al., 1977), phyllaemblicins A–F and G1–G8 from *Phyllanthus emblica* Linn (Lv et al., 2014a; Zhang et al., 2000a,b, 2001), and phyllanthacidoids A–U from *Phyllanthus acidus* Skeels (Lv et al., 2014b; Vongvanich et al., 2000) have been previously reported. These compounds showed potent antileukemic (Kupchan et al., 1977), cytotoxic (Vongvanich et al., 2000) and anti-viral (Liu et al., 2009; Lv et al., 2014a,b) activities, which attracted considerable attention by pharmacologists and organic chemists (Moore and Powis, 1986; Smith et al., 1991).

Phyllanthus emblica Linn. is an important medicinal plant that has been described in Chinese herbal medicine (called Yu Gan Zi), Ayurvedic medicine, and Tibetan medicine. Its roots are used for treatment of hypertension and enteritis in China (Xie, 1996). Continued studies on the chemical composition of this plant led herein to identification of 14 new sesquiterpenoid glycosides, along with three known ones. Their structures featured phyllaemblic acid (**1a**) as the aglycone connected to different sugar moieties, e.g., glucopyranosyl, xylopyranosyl, arabinopyranosyl, 6-deoxyglucopyranosyl, and/or *myo*-inositol units were determined on the basis of detailed spectroscopic analysis. A pre-column derivative/chiral separation/DAD detection method was established and applied to determine the absolute configurations of the sugar parts of the new glycosides. Quantum chemical calculated electronic circular dichroism (ECD) using time-dependent density functional theory (TDDFT) was used to elucidate the absolute configurations of the aglycone. Moreover, the antiviral activities of the isolated compounds against enterovirus 71 (EV71) for hand, foot and mouth disease, influenza A virus strain H3N2, herpes simplex virus (HSV-1), and Coxsackie virus B3 (CVB3), as well as their cytotoxic activities against human cancer cell lines, were evaluated. Herein, the results obtained in this study were presented.

* Corresponding authors.
E-mail addresses: xumin@mail.kib.ac.cn (M. Xu), zhangyj@mail.kib.ac.cn (Y.-J. Zhang).
[1] These authors contributed equally to this article.

http://dx.doi.org/10.1016/j.phytochem.2015.06.001
0031-9422/

2. Results and discussion

Taking into account the high contents of tannins and sugars in the 70% ethanolic extract of the air-dried *P. emblica* roots, Diaion HP20SS column chromatography (CC) was first used to remove sugars and to enrich the sesquiterpenoid glycoside (50–80% CH_3OH in H_2O) fraction. Silica gel CC was then employed to remove most of the tannins and to fractionate the sesquiterpenoid glycoside. Then, Sephadex LH-20 CC of the sesquiterpenoid glycoside fraction eluted with a CH_3OH/H_2O gradient system further enriched the sesquiterpenoid glycosides (0–30% CH_3OH in H_2O). The enriched target fractions were next further purified by passage over MCI-gel CHP20P, Toyopearl HW-40C and RP-8, followed by preparative HPLC (p-HPLC) to afford 17 compounds (**1**–**17**), respectively, with purification guided by thin layer chromatography (TLC) and HPLC-DAD analyses. The new compounds **1**–**14** were all norbisabolane type sesquiterpenoid glycosides with phyllaemblic acid as the aglycone (Fig. 1). Three known sesquiterpenoid glycosides were determined to be phyllaemblicins B (**15**) (Zhang et al., 2000a) and C (**16**) (Zhang et al., 2000a), and glochicoccinoside D (**17**) (Xiao et al., 2007), respectively, by comparing with authentic samples directly and their spectroscopic and physical data with those previously reported in literatures.

2.1. Structure elucidations of new compounds

Phyllaemblicin H1 (**1**) was obtained as a white amorphous powder, with a molecular formula of $C_{35}H_{46}O_{20}$, as established from HRESIMS *m/z* 831.2556 $[M+HCOO]^-$. Its ^1H NMR spectrum (Table 1) showed characteristic signals arising from a benzoyl group (δ_H 8.17, 7.54, and 7.64), an acetyl methyl group (δ_H 2.10, s, 3H), one methyl group at δ_H 0.90 (3H, d, J = 6.8 Hz), and two anomeric protons of two sugar units [δ_H 5.57 (1H, d, J = 8.2 Hz), and δ_H 4.21 (1H, d, J = 7.6 Hz)]. In its ^{13}C NMR spectrum (Table 1), apart from the resonances of one benzoyl and two hexosyl groups, 14 carbon signals arising from one methyl (δ_C 13.3), four methylenes including one oxygen-bearing one (δ_C 63.6), five methines (three oxymethines), one ketal carbon (δ_C 100.6), one carboxyl (δ_C 175.9), one oxygen bearing quaternary carbon (δ_C 75.7), and one carbonyl (δ_C 213.8) were observed. The aforementioned data indicated that **1** was a highly oxygenated bisabolane sesquiterpenoid glycoside (Zhang et al., 2000b). These NMR features were comparable to those of phyllaemblicin B, a known highly oxygenated norbisabolane glycoside isolated from the title plant (Zhang et al., 2000a), except for an additional acetyl group. Based on the HMBC correlation (Fig. 2) of H-6″ of the inner glucosyl to the acetyl δ_C 172.8 (C-1‴′), it was determined that compound **1** was 6″-acetyl phyllaemblicin B.

Phyllaemblicin H2 (**2**) had the same molecular formula as **1**, deduced from the HRESIMS. The NMR spectroscopic data (Table 1) of **2** were similar to **1**. Extensive analysis of the 2D NMR spectra indicated that **2** was also an acetylated derivative of phyllaemblicin B. The HMBC correlation between the terminal glucosyl H-6‴ (δ_H 4.17) to δ_C 173.1 allowed the connection of the acetyl group to C-6‴ of the terminal glucosyl. Accordingly, compound **2** was determined to be 6‴-acetyl phyllaemblicin B.

Both phyllaemblicins H3 (**3**) and H4 (**4**) had a disaccharide moiety. One of the sugars was assigned as a glucopyranosyl [anomeric proton at δ_H 5.58, d, J = 8.2 Hz for **3** and δ_H 4.20, d, J = 7.6 Hz for **4**] unit, on the basis of 1D and 2D NMR spectra. Another sugar moiety was a xylopyranosyl (anomeric proton at δ_H 3.95, d, J = 7.7 Hz) for **3** and an arabinopyranosyl (anomeric proton at δ_H 5.50, d, J = 7.7 Hz) for **4**. The monosaccharides in **3** and **4** were further confirmed by acid hydrolysis followed by pre-column derivatization/chiral separation/DAD detection (Fig. 3). After acid hydrolysis, the

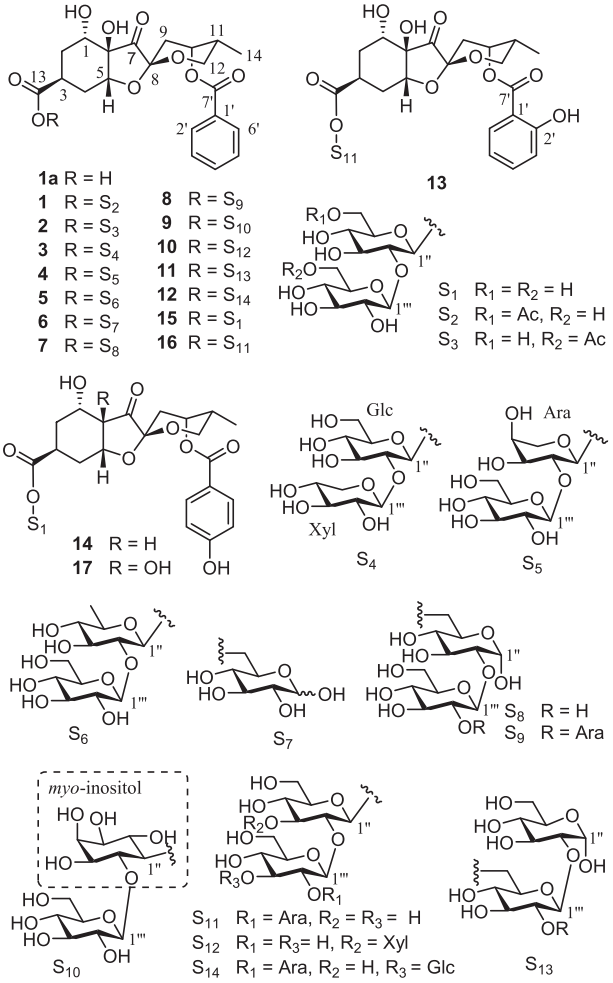

Fig. 1. Structures of compounds from *P. emblica*.

reaction of monosaccharides with 1-phenyl-3-methyl-5-pyrazolone (PMP) in 0.3 M NaOH solution at 70 °C was carried out (Honda et al., 1989). After chiral HPLC separation, the monosaccharides were determined to be D-glucose and D-xylose for **3**, and D-glucose and L-arabinose for **4**, by comparing their retention times (t_R) with the corresponding standards D-glucose (t_R, 15.0 min), D-xylose (t_R, 15.5 min) and L-arabinose (t_R, 11.3 min) (Fig. 3).

The sugar moiety of phyllaemblicin H5 (**5**) comprised of two hexosyl units, including one glucosyl unit. Two anomeric protons at δ_H 5.52 (1H, d, J = 8.1 Hz, H-1″) and 4.19 (1H, d, J = 8.0 Hz, glucosyl H-1) were observed in the ^1H NMR spectrum (Table 2). All of the proton and carbon signals from the two hexosyl units were unambiguously assigned by HSQC-TOCSY experiments. Besides the proton spin system of the glucosyl moiety, the proton spin system of H-1″/H-2″/H-3″/H-4″/H-5″/H-6″ was constructed for another hexosyl unit. The presence of the methyl signal [δ_C 18.2 and δ_H 1.33] and the large coupling constants (Table 2) of H-1″ to H-4″ indicated that this monosaccharide was a 6-deoxy β-glucopyranosyl unit. In the HMBC spectrum of **5**, the correlations from H-1″ to the carboxyl carbon of the aglycone at δ_C 176.1, and H-1‴ to C-2″ confirmed the connectivity of the disaccharide moiety. Using the same method as described for **3** and **4**, the glucosyl unit in **5** was determined to have a D configuration (rt = 15.0 min), while the absolute configurations of the 6-deoxy β-glucosyl unit (t_R, 15.7 min) were not determined due to the lack of an authentic sample.

The MS and ^{13}C NMR spectra of phyllaemblicin H6 (**6**) indicated that there was only one hexosyl unit. However, two anomeric proton signals [δ_H 5.11 (d, J = 3.8 Hz) and 4.52 (d, J = 7.8 Hz)] with one

Table 1
^{13}C and ^{1}H NMR Spectroscopic data for compounds **1**–**4** in CD_3OD (δ in ppm).

No.	1		2		3		4	
	δ_C	δ_H	δ_C	δ_H	δ_C	δ_H	δ_C	δ_H
1	71.6, CH	3.92 brs	71.4, CH	3.91 brs	71.2, CH	3.91 brs	71.4, CH	3.94 brs
2	32.5, CH_2	1.74 ddd (2.5, 13.0, 14.0) 2.05[a]	32.7, CH_2	1.77 ddd (2.5, 13.0 14.0) 1.95[a]	32.5, CH_2	1.76 ddd (2.5, 13.0 14.0) 1.89[a]	32.3, CH_2	1.77 ddd (2.5, 13.0, 14.0) 2.04 brd (14.0)
3	32.3, CH	2.88 tt (3.0, 13.0)	32.5, CH	2.94 tt (3.0, 13.0)	32.3, CH	2.95 tt (3.0, 13.0)	32.2, CH	2.93 tt (3.0, 13.0)
4	29.4, CH_2	1.88 ddd (3.7, 13.0, 14.6) 2.31 brd (3.9, 14.6)	29.4, CH_2	1.89 ddd (3.8, 13.0, 14.6) 2.36 brd (14.6)	29.4, CH_2	1.87[a] 2.35 brd (14.4)	29.2, CH_2	1.90 ddd (4.0, 13.0, 14.5) 2.34 brd (14.5)
5	76.3, CH	4.28[a]	76.4, CH	4.28 brs	76.3, CH	4.27 brs	76.4, CH	4.31 brs
6	75.7, C		75.7, C		75.7, C		75.5, C	
7	213.8, C		213.8, C		214.0, C		213.7, C	
8	100.6, C		100.6, C		100.6, C		100.6, C	
9	32.8, CH_2	1.98 dd (3.0, 14.9) 2.31[a]	32.9, CH_2	2.00 dd (3.0, 14.6) 2.30 dd (3.5, 14.6)	32.8, CH_2	1.98 dd (3.5, 15.0) 2.31 dd (3.5, 15.0)	32.7, CH_2	2.02 dd (3.4, 15.0) 2.32 dd (3.4, 15.0)
10	71.2, CH	5.34 brs	71.2, CH	5.36 brs	71.1, CH	5.34 brs	71.0, CH	5.38 brs
11	34.4, CH	2.18 m	34.5, CH	2.18 m	34.3, CH	2.17 m	34.3, CH	2.20 m
12	63.6, CH_2	3.58[a] 4.05 dd (11.5, 11.5)	63.5, CH_2	3.56 dd (4.6, 11.5) 4.01 dd (11.5, 11.5)	63.4, CH_2	3.57[a] 4.05 dd (11.5, 11.5)	63.4, CH_2	3.60 dd (4.0, 11.5) 4.06 dd (11.5, 11.5)
13	175.9, C		176.3, C		175.9, C		175.8, C	
14	13.3, CH_3	0.90 d (6.8)	13.3, CH_3	0.89 d (6.9)	13.1, CH_3	0.89 d (6.9)	13.1, CH_3	0.92 d (6.9)
1′	132.4, C		132.4, C		132.2, C		132.2, C	
2′,6′	131.0, CH	8.17 d (8.0)	131.0, CH	8.17 d (8.0)	130.8, CH	8.17 d (8.0)	130.9, CH	8.20 d (8.0)
3′,5′	130.0, CH	7.54 t (8.0)	130.1, CH	7.57 t (8.0)	130.0, CH	7.57 t (8.0)	129.7, CH	7.57 t (8.0)
4′	134.5, CH	7.64 t (8.0)	134.6, CH	7.66 t (8.0)	134.5, CH	7.65 t (8.0)	134.8, CH	7.65 t (8.0)
7′	168.0, C		167.8, C		167.9, C		167.8, C	
1″	93.7, CH	5.57 d (8.2)	93.9, CH	5.59 d (8.1)	94.0, CH	5.58 d (8.2)	94.4, CH	5.50 d (7.7)
2″	82.8, CH	3.42 dd (8.2, 9.2)	82.6, CH	3.45 dd (8.1, 9.0)	84.0, CH	3.28 dd (8.2, 9.0)	82.7, CH	3.44 dd (7.7, 8.4)
3″	77.9, CH	3.62 dd (9.2, 9.2)	78.1, CH	3.63 dd (9.0, 9.0)	77.6, CH	3.57 dd (9.0, 9.0)	77.3, CH	3.60 brd (8.4)
4″	70.9, CH	3.46 dd (9.2, 9.2)	70.8, CH	3.45 dd (9.0, 9.0)	70.8, CH	3.43 dd (9.0, 9.0)	70.6, CH	3.63 m
5″	76.3, CH	3.60 m	79.0, CH	3.39 m	78.9, CH	3.38 m	67.5, CH_2	3.34[a] 3.95 dd (3.9, 11.4)
6″	64.5, CH_2	4.28[a] 4.42 dd (2.0,12.3)	62.3, CH_2	3.73 dd (5.2, 12.3) 3.87 dd (2.3,12.3)	62.2, CH_2	3.74 dd (5.0, 12.0) 3.88 dd (2.0,12.0)		
1‴	106.0, CH	4.21 d (7.6)	105.7, CH	4.29 d (7.8)	106.9, CH	3.95 d (7.7)	105.8, CH	4.20 d (7.6)
2‴	76.0, CH	3.11 dd (7.6, 9.1)	76.0, CH	3.13 dd (7.8, 9.0)	75.9, CH	3.07 dd (7.7, 9.1)	75.8, CH	3.14 dd (7.6, 9.2)
3‴	78.0, CH	3.24 dd (9.1, 9.1)	77.6, CH	3.27 dd (9.0, 9.0)	77.5, CH	3.18 dd (9.1, 9.1)	77.7, CH	3.27 dd (9.2, 9.2)
4‴	71.2, CH	3.23 m[a]	71.2, CH	3.22 dd (9.0, 9.0)	71.0, CH	3.31[a]	70.7, CH	3.27 m
5‴	77.9, CH	2.82 ddd (2.1, 4.3, 9.2)	75.4, CH	3.09 m	67.1, CH_2	2.83 dd (11.1, 11.1) 3.70 dd (5.3, 11.1)	77.7, CH	2.81 ddd (2.3, 4.2, 9.6)
6‴	62.1, CH_2	3.58 m	64.6, CH_2	4.17 m			62.0, CH_2	3.59 dd (5.3, 12.3) 3.65 dd (2.2, 12.3)
$\underline{CH_3}CO$	21.0, CH_3	2.10 s	21.0, CH_3	1.98 s				
$CH_3\underline{CO}$	172.8, C		173.1, C					

Data were recorded at 150 MHz for ^{13}C and 600 MHz for ^{1}H.
[a] Overlapped.

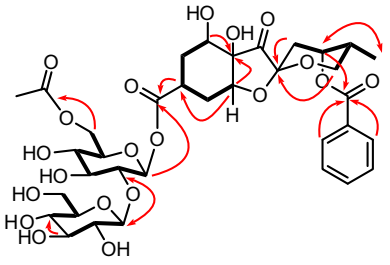

Fig. 2. ^{1}H–^{1}H COSY (—) and HMBC (→) correlations of **1**.

proton integral suggested that the hexosyl moiety existed as a mixture of α and β isomers. In the ^{1}H–^{1}H COSY spectrum, a proton spin system of δ_H 5.11 (H-1″)/H-2″/H-3″/H-4″/H-5″/H-6″ was constructed for the α-isomer. The large coupling constants (Table 2) for H-2″, H-3″, and H-5″ suggested that it was an α-glucopyranosyl. In the same way, the resonances for the β-isomer were also completely assigned. The down-field chemical shift (δ_C 65.0) suggested that C-6″ in the glucosyl group was substituted. This was further confirmed by HMBC correlations from H-6″ to C-13 of the aglycone. Therefore, the glucosyl moiety in **6** was attached to C-13 through the C-6″ hydroxyl group.

Compared to **6**, phyllaemblicin H7 (**7**) had one more glucopyranosyl unit (anomeric proton at δ_H 4.51, 1H, d, J = 7.5 Hz, H-1‴) attached to the inner glucosyl C-2″. This was confirmed by the HMBC correlation from H-1‴ to C-2″. As for **8**, it had one more arabinopyranosyl (δ_C 107.5, δ_H 4.50, 1H, d, J = 8.2 Hz) unit than compound **7**, based on extensive analysis of HSQC-TOCSY and ^{1}H-^{1}H COSY spectra. The additional arabinosyl group in **8** was connected to C-2‴ of the middle glucosyl, taking into account the HMBC correlation from H-1⁗ to C-2‴. The anomeric free glucosyl unit in both **7** and **8** mainly existed as α-form (Tables 2 and 3), due to the substitution at the C-2 position.

Phyllaemblicin H9 (**9**) had the same molecular formula $C_{33}H_{44}O_{19}$ as phyllaemblicin B (**15**), on the basis of HRESIMS. However, the ^{1}H NMR spectrum (Table 3) of **9** displayed only one anomeric proton for β-glucopyranosyl (δ_H 3.91, 1H, d, J = 7.8 Hz, H-1‴). H-1″ was assigned at δ_H 4.83 based on its HMBC correlation with C-13 of the aglycone. This oxymethine proton (δ_H 4.83) was obviously involved in the proton spin system for (H-1″)/H-2″/H-3″/H-4″, and H-1″/H-6″/H-5″. Together with the HMBC correlations from H-3″ to C-4″ and from H-4″ to C-2″, an inositol moiety could be constructed, whose relative configuration was determined by its coupling constants from H-1″ to H-6″ (Table 3) and it was assigned as *myo*-inositol. The HMBC correlation from H-1‴ to C-2″

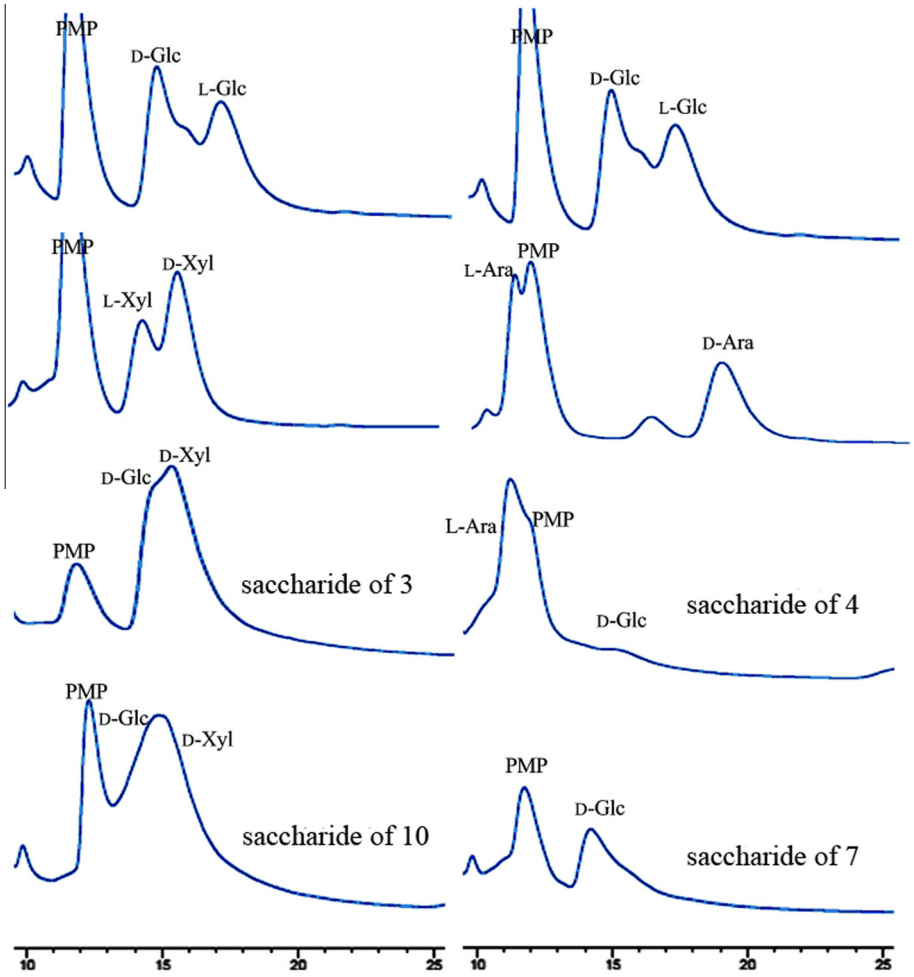

Fig. 3. HPLC chromatograms of chiral separation of monosaccharides from hydrolysis of compounds **3**, **4**, **7** and **10**. (PMP: 1-phenyl-3-methyl-5-pyrazolone).

confirmed that the terminal glucosyl unit was connected to *myo*-inositol C-2″. Accordingly, the saccharide part of **9** was elucidated as *myo*-inositol-2-*O*-*β*-glucopyranosyl.

The MS and NMR data (Table 3) of phyllaemblicin H10 (**10**) indicated the presence of two hexosyl and one pentosyl units, including two glucopyranosyl [anomeric protons at δ_H 5.63 and 4.53 (each 1H)] and one xylopyranosyl (anomeric proton at δ_H 4.63 (1H, d, J = 7.5 Hz)) moieties, which was confirmed by HSQC-TOCSY and ^{1}H–^{1}H COSY experiments. The HMBC correlation from one glucosyl anomeric proton at δ_H 5.63 to the aglycone C-13 (δ_C 175.7) allowed assignment of this glucosyl at the inner position. The chemical shifts of the inner glucosyl C-2″ and C-3″ shifted to δ_C 79.8 and 87.7, suggesting that both C-2″ and C-3″ in **10** were substituted. In the HMBC spectrum, the signals of H-1‴ (δ_H 4.53) of the second glucosyl group and H-1⁗ (δ_H 4.63) of the xylosyl group were correlated with the inner glucosyl C-2″ (δ_C 79.8) and C-3″ (δ_C 87.7), respectively. Based on the above evidence, the sugar moiety of **10** was elucidated as S12. Acid hydrolysis followed by chiral separation analysis further determined the absolute configuration of the monosaccharides as D-glucose and D-xylose, which were the same as those for **3** (Fig. 3).

Phyllaemblicin H11 (**11**) had the same molecular formula $C_{33}H_{44}O_{19}$ as **7**. The 1D NMR spectra were also comparable to those of **7**. In the HMBC spectrum, the signal of H-6″ (δ_H 4.23 and 4.38) of one glucosyl unit showed correlations with the aglycone C-13 (δ_C 175.9). According to the HSQC-TOCSY and ^{1}H–^{1}H COSY correlations, the proton spin system of δ_H 4.23 and 4.38 (H-6″)/H-5″/H-4″/H-3″/H-2″/H-1″ was established, and the inner *β*-glucosyl was constructed. The terminal glucopyranosyl unit with an α anomeric center was also constructed. On the basis of the HMBC correlation from H-1″ to the C-2‴ (δ_C 82.7), the sugar moiety of **11** was determined as S_{13}.

The 1D NMR spectra and HRMS of phyllaemblicin H12 (**12**) indicted that the sugar moiety was comprised of three hexosyl and one pentosyl units. Based on the HSQC-TOCSY and ^{1}H–^{1}H COSY spectra measured on an 800 MHz NMR spectrometer, four proton spin systems for three *β*-glucopyranosyl and one α-arabinopyranosyl groups were successfully constructed (Fig. 4), whose corresponding carbon signals were also unambiguously assigned. In the HMBC spectrum of **12**, H-1″ (δ_H 5.60, d, J = 8.0 Hz) of the inner glucosyl, H-1‴ (δ_H 4.14, d, J = 8.0 Hz) of the middle glucosyl, H-1⁗ (δ_H 4.64, d, J = 8.0 Hz) of the terminal arabinosyl, and H-1⁗′ (δ_H 4.62, d, J = 8.0 Hz) of the terminal glucosyl were correlated respectively with C-13 (δ_C 175.9) of the aglycone, C-2″ (δ_C 84.0) of the inner glucosyl, C-2‴ (δ_C 82.4) and C-3‴ (δ_C 87.0) of the middle glucosyl. Thus, the sugar moiety in **12** was constructed as S_{14}.

Phyllaemblicins H1–H12 (**1**–**12**) had the same aglycone as phyllaemblic acid, whose relative configurations were established on the basis of their proton coupling constants and ROESY correlations (Zhang et al., 2000b). Taking compound **5** as an example, the small coupling constants of H-1 and H-5 suggested both protons were in an equatorial orientation. The coupling constants of H-3 (tt, J = 3.0, 13.0 Hz) indicated that H-3 was axially orientated. In the chair

Table 2
^{13}C and ^{1}H NMR Spectroscopic data for compounds **5**–**7** in CD_3OD (δ in ppm).

No.	**5**		**6**[b]				**7**	
	δ_C[a]	δ_H[c]	δ_C		δ_H		δ_C[a]	δ_H[c]
1	71.6, CH	3.92 brs	71.1, CH		3.92 brs		71.6, CH	3.92 brs
2	32.5, CH_2	1.74 ddd (2.5, 13.0 14.5) 1.99 dd (3.0, 14.5)	33.1, CH_2		1.74 ddd (2.5, 13.0, 14.5) 1.96 brd (14.5)		33.1, CH_2	1.74 ddd (2.5, 12.5, 14.0) 1.95 m
3	32.3, CH	2.90 tt (3.0, 13.0)	32.1, CH		2.85 m		32.1, CH	2.86 tt (3.5, 12.5)
4	29.4, CH_2	1.89 ddd (4.0, 13.0, 14.5) 2.32[d]	28.8, CH_2		1.90[d] 2.32[d]		28.8, CH_2	1.90 ddd (3.7, 13.0, 14.8) 2.33 m
5	76.4, CH	4.28 brs	76.3, CH		4.30 brs		76.4, CH	4.28 brs
6	75.6, C		75.6, C				75.6, C	
7	213.8, C		213.8, C				213.9, C	
8	100.7, C		100.5, C				100.5, C	
9	32.8, CH_2	1.97 dd (3.5, 14.5) 2.30 dd (3.5, 14.5)	32.6, CH_2		2.00 dd (1.5, 15.0) 2.31[d]		32.5, CH_2	1.99 dd (2.5, 14.5) 2.32 m
10	71.2, CH	5.34 brs	71.1, CH		5.35 brs		71.1, CH	5.36 brs
11	34.5, CH	2.17 m	34.2, CH		2.21 m		34.3, CH	2.19 m
12	63.6, CH_2	3.57[a] 4.03 dd (11.5, 11.5)	63.4, CH_2		3.62 dd (4.4, 11.3) 4.05 dd (11.3, 11.3)		63.4, CH_2	3.60[d] 4.04 dd (11.4, 11.4)
13	176.1, C		177.1, C				177.2, C	
14	13.3, CH_3	0.89 d (6.9)	13.1, CH_3		0.94 d (6.9)		13.1, CH_3	0.99 d (6.9)
1′	132.2, C		132.0, C				132.0, C	
2′,6′	131.0, CH	8.16 d (8.0)	130.9, CH		8.16 d (8.2)		130.8, CH	8.17 d (8.0)
3′,5′	130.0, CH	7.53 t (8.0)	129.6, CH		7.60 t (8.2)		129.7, CH	7.57 t (8.0)
4′	134.5, CH	7.63 t (8.0)	134.4, CH		7.65 t (8.2)		134.4, CH	7.65 t (8.0)
7′	168.2, C		168.0, C				168.0, C	
			α	β	α	β		
1″	93.8, CH	5.52 d (8.1)	93.9, CH	98.3, CH	5.11 d (3.8)	4.52 d (7.8)	93.6, CH	5.38 d (3.5)
2″	83.4, CH	3.40 dd (8.1, 9.0)	73.8, CH	76.1, CH	3.37 dd (3.8, 9.3)	3.16 dd (7.8, 9.2)	83.0, CH	3.48 dd (3.5, 9.5)
3‴	77.8, CH	3.55 dd (9.0, 9.0)	74.7, CH	77.8, CH	3.71 dd (9.3, 9.3)	3.37 dd (9.2, 9.2)	73.6, CH	3.88 dd (9.5, 9.5)
4″	76.1, CH	3.11 dd (9.0, 9.0)	71.5, CH	71.3, CH	3.31[d]	3.31[d]	71.4, CH	3.38[d]
5″	74.5, CH	3.42 m	70.7, CH	75.4, CH	3.99 ddd (2.0, 5.3, 9.3)	3.48 ddd (2.1, 5.6, 9.2)	70.7, CH	4.00 ddd (2.0, 5.0, 9.7)
6″	18.2, CH_2	1.33 d (6.3)	65.0, CH_2	65.0, CH_2	4.32 dd (2.0, 11.9) 4.25 dd (5.3, 11.9)	4.21 dd (2.1, 11.9) 4.36 dd (5.7, 11.9)	64.8, CH_2	4.32 dd (2.0, 11.8) 4.26 dd (5.0, 11.8)
1‴	106.1, CH	4.19 d (8.0)					106.0, CH	4.51 d (7.5)
2‴	76.5, CH	3.09 dd (8.0, 8.8)					75.4, CH	3.30 dd (7.5, 9.0)
3‴	77.9, CH	3.23 m					77.9, CH	3.31[d]
4‴	70.9, CH	3.23 m					71.4, CH	3.34 dd (9.0, 9.0)
5‴	78.0, CH	2.78 ddd (2.3, 4.3, 9.5)					77.9, CH	3.31[d]
6‴	63.6, CH_2	3.56[d] 3.62[d]					62.6, CH_2	3.68 dd (5.0, 12.0) 3.87 dd (2.5, 12.0)

[a] Data were recorded at 100 MHz.
[b] Data were recorded at 600 MHz for ^{1}H NMR and 150 MHz for ^{13}C NMR.
[c] Data were recorded at 800 MHz.
[d] Overlapped.

conformation of the A ring (Fig. 5), H-3 was located at the opposite face of H-1 and H-5. This was confirmed by the ROESY correlations of H-3 with H-2 eq (δ_H 1.99) and H-4 eq (δ_H 2.32), and strong ROESY correlations of H-1 with H-2ax, and H-5 with H-4ax. The large coupling constant (11.5 Hz) of $J_{H\text{-}12,H\text{-}11}$ indicated an axial orientation of H-11, and a broad singlet of H-10 suggested its equatorial orientation locating at the same side as H-11 in a chair shaped tetrahydropyran ring C. Together with the ROESY correlations of H-4 eq and H-3 with the benzoyl aromatic protons (δ_H 8.16), the relative configurations of the aglycone of **5** were established as shown in Fig. 5.

The absolute configurations of compounds **1**–**12** were determined by comparing their experimental ECD curves with the experimental and calculated ECD curves of phyllaemblic acid (Fig. 6). The conformer search was carried out using the mechanics MMFF method. The resulting conformers (<20 kJ/mol) were re-optimized using DFT at the B3LYP-SCRF/6-311G (d,p) level. Ten of the conformers with energy <2 kcal/mol were considered for ECD calculation. These lower energy conformers differed in the orientations of the benzoyl moiety (Supplementary S-108 Fig. 4). The calculated ECD spectra of the conformers were similar and comparable to the averaged ECD spectrum (Supplementary S-108 Fig. 5). The Cotton effects at 230 nm and 250 nm were produced by π–π^* excitation of the benzoate moiety, and their signs were determined by the configuration at C*-10. The strong negative Cotton effect at 320 nm was produced by the n–π^* excitation of the carbonyl (C-7) group, which was adjacent to the stereo centers of C*-6 and C*-8. The experimental ECD curves agreed well with the calculation results. Thus, the absolute configurations of the aglycone moiety of compounds **1**–**12** were determined as 1*S*, 3*S*, 5*R*, 6*R*, 8*S*, 10*S*, 11*R*.

Phyllaemblicin H13 (**13**) was obtained as a white powder, possessing a molecular formula of $C_{38}H_{52}O_{24}$, as established from the HRESIMS. Its NMR spectra (Table 4) resembled phyllaemblicin C (**16**), except for signals arising from a benzoyl moiety. The mutually coupled four aromatic proton signals at δ_H 7.03 (1H, dd, J = 1.0, 8.0 Hz, H-3′), 7.59 (1H, ddd, J = 1.8, 8.0, 8.4 Hz, H-4′), 7.06 (1H, ddd, J = 1.0, 8.0, 8.4 Hz, H-5′), and 8.12 (1H, dd, J = 1.8, 8.0 Hz, H-6′) established a 2-hydroxyl benzoyl moiety in **13**, instead of a benzoyl moiety in **16**. The relative configuration of **13** was established by ROESY correlations and coupling constants as for **5**, and the absolute configuration was determined by ECD calculations. Due to the different substitution in the benzoyl moiety, the ECD curve of **13** differed from phyllaemblic acid. Though the experimental ECD curve of **13** and the calculated ECD curve of the aglycone of **13** did not match very well at 280–300 nm, there was a weak peak at 287 nm in the experimental spectrum corresponding to the peak between 280 and 300 nm in the calculated ECD curve (Fig. 7 left). This was confirmed by comparing the

Table 3
^{13}C and ^{1}H NMR Spectroscopic data for compounds **8**–**11** in CD_3OD (δ in ppm).

No.	**8**		**9**[b]		**10**[a]		**11**	
	δ_C[a]	δ_H[c]	δ_C	δ_H	δ_C	δ_H	δ_C[b]	δ_H[c]
1	71.5, CH	3.91 brs	71.8, CH	3.93 brs	71.6, CH	3.94 brs	71.2, CH	3.92 brs
2	33.1, CH_2	1.73 ddd (1.9, 13.0, 14.6)	31.6, CH_2	1.78 ddd (3.0, 13.0 15.2)	32.2, CH_2	1.79 ddd (2.5, 13.1, 14.5)	33.0, CH_2	1.76 ddd (2.7, 13.0, 14.0)
		1.92[d]		2.00[d]		2.06 dd (2.5, 14.5)		1.98 dd (3.2, 14.0)
3	32.2, CH	2.84 m	32.2, CH	2.92 tt (2.4, 13.0)	32.3, CH	2.91 tt (3.0, 13.1)	32.1, CH	2.83 tt (3.3, 13.0)
4	28.8, CH_2	1.90[d]	29.8, CH_2	1.87 ddd (3.4, 13.0, 14.4)	29.3, CH_2	1.92 ddd (3.6, 13.1, 14.5)	29.0, CH_2	1.93 ddd (3.3, 13.0, 14.3)
		2.30[d]		2.62 brd (14.4)		2.35 brd (14.5)		2.28 brd (14.3)
5	76.3, CH	4.25 brs	76.7, CH	4.33 brs	76.3, CH	4.31 brs	76.4, CH	4.29 brs
6	75.6, C		75.6, C		75.5, C		75.7, C	
7	213.7, C		213.9, C		213.9, C		213.8, C	
8	100.6, C		100.6, C		100.6, C		100.5, C	
9	32.5, CH_2	1.97[d]	32.9, CH_2	2.04 dd (2.4, 15.0)	32.7, CH_2	2.03 dd (4.0, 14.6)	32.4, CH_2	1.99 dd (3.4, 14.9)
		2.30[d]		2.26 dd (3.7, 15.0)		2.28 dd (3.0, 14.6)		2.35 dd (3.3, 14.9)
10	71.2, CH	5.33 brs	70.9, CH	5.37 brs	71.0, CH	5.39 brs	71.2, CH	5.33 dd (3.3, 6.4)
11	34.3, CH	2.18[d]	34.4, CH	2.20 m	34.3, CH	2.20[d]	34.3, CH	2.21[d]
12	63.5, CH_2	3.57[d]	63.4, CH_2	3.62[d]	63.5, CH_2	3.59[d]	63.6, CH_2	3.62[d]
		4.01[d]		4.07 dd (11.4, 11.4)		4.06 dd (11.4, 11.4)		4.04 dd (11.1, 11.1)
13	177.3, C		176.9, C		175.7, C		175.9, C	
14	13.0, CH_3	0.91 d (6.8)	13.1, CH_3	0.89 d (7.1)	13.1, CH_3	0.92 d (7.0)	13.1, CH_3	0.95 d (7.1)
1′	132.1, C		132.1, C		132.1, C		132.1, C	
2′,6′	130.7, CH	8.14 d (8.0)	131.0, CH	8.21 d (8.3)	130.8, CH	8.18 d (8.0)	129.6, CH	8.17 d (8.2)
3′,5′	129.6, CH	7.53 d (8.0)	130.0, CH	7.61 t (8.3)	129.9, CH	7.58 t (8.0)	130.9, CH	7.55 t (8.2)
4′	134.4, CH	7.64 t (8.0)	134.9, CH	7.86 t (8.3)	134.5, CH	7.68 t (8.0)	134.4, CH	7.68 t (8.2)
7′	168.1, C		167.9, C		167.9, C		167.9, C	
1″	93.5, CH	5.33 d (3.2)	75.1, CH	4.83 dd (9.6, 9.6)	93.9, CH	5.63 d (8.0)	105.9, CH	4.51 d (7.8)
2″	84.4, CH	3.37[d]	83.9, CH	3.78 dd (9.6, 9.6)	79.8, CH	3.67 dd (8.0, 9.0)	75.2, CH	3.32 dd (7.8, 9.7)
3″	73.4, CH	3.85 dd (9.4, 9.4)	73.6, CH	3.61 dd (2.6, 9.6)	87.7, CH	3.76[d]	77.7, CH	3.41 dd (9.7, 9.7)
4″	71.2, CH	3.39[d]	73.4, CH	4.08 dd (2.6, 2.6)	69.5, CH	3.52 dd (9.0, 9.0)	71.8, CH	3.28 dd (9.7, 9.7)
5″	70.8, CH	3.95 ddd (2.3, 5.4, 9.6)	73.5, CH	3.47 dd (2.6, 9.6)	78.4, CH	3.44 m	75.5, CH	3.48 ddd (2.1, 7.2, 9.7)
6″	64.8, CH_2	4.26 m	72.7, CH_2	3.93 dd (9.6, 9.6)	62.2, CH_2	3.77[d]	64.5, CH_2	4.23 dd (7.2, 11.8)
						3.92 dd (1.5, 12.1)		4.38 dd (2.1, 11.8)
1‴	105.1, CH	4.54 d (8.2)	106.5, CH	3.91 d (7.8)	104.3, CH	4.53 d (8.0)	93.8, CH	5.27 d (3.6)
2‴	85.4, CH	3.42 dd (8.2, 9.1)	75.8, CH	3.08 dd (7.8, 9.4)	75.6, CH	3.04 dd (8.0, 9.0)	82.7, CH	3.39 dd (3.6, 9.3)
3‴	77.5, CH	3.55 dd (9.1, 9.1)	78.2, CH	3.16 dd (9.4, 9.4)	78.2, CH	3.23 dd (9.0, 9.0)	73.6, CH	3.86 dd (9.3, 9.3)
4‴	71.2, CH	3.38[d]	70.4, CH	3.24 dd (9.4, 9.4)	71.0, CH	3.26[d]	71.6, CH	3.38[d]
5‴′	77.7, CH	3.29 dd (2.5, 5.5, 9.1)	77.3, CH	2.36 m	77.3, CH	2.84 ddd (2.4, 4.2, 9.0)	72.9, CH	3.79 ddd (2.5, 6.9, 9.4)
6‴	62.5, CH_2	3.66[d]	61.6, CH_2	3.39[d]	62.3, CH_2	3.55[d]	62.5, CH_2	3.71[d]
		3.83[d]		3.50 dd (2.8, 12.7)		3.61[d]		3.79[d]
1⁗	107.5, CH	4.50 d (8.2)			105.1, CH	4.63 d (7.5)		
2⁗	73.7, CH	3.65[d]			75.4, CH	3.29[d]		
3⁗	74.3, CH	3.56 dd (4.8, 9.3)			78.4, CH	3.31[d]		
4⁗	69.5, CH	3.81 brs			71.2, CH	3.28[d]		
5⁗	67.7, CH_2	3.64[d]			67.2, CH_2	3.28[d]		
		3.98[d]				3.94[d]		

[a] Data were recorded at 125 MHz for ^{13}C or 500 MHz for ^{1}H.
[b] Data were recorded at 150 MHz for ^{13}C or 600 MHz for ^{1}H.
[c] Data were recorded at 800 MHz.
[d] Overlapped.

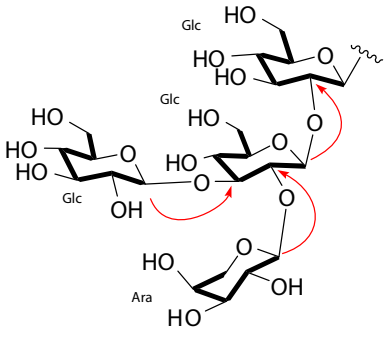

Fig. 4. Key ^{1}H–^{1}H COSY (—) and HMBC (→) correlations of S14.

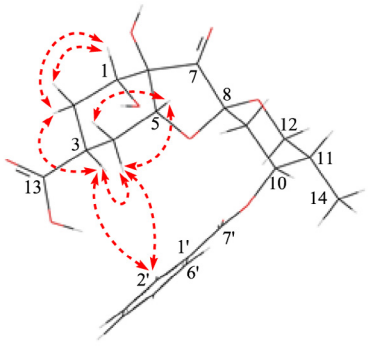

Fig. 5. Key ROESY correlations in the lowest energy conformer of **5**.

experimental CD curve of **13** with those of phyllaemblic acid, **7** and **10** with the benzoyl chromophore (Fig. 7 right). It is obvious that the TDDFT computation overestimated the intensity of the peak at 280–300 nm. However, it could still predict the tendency of the experimental ECD curve between 280 and 300 nm. Thus, the absolute configuration of **13** was determined (Fig. 7).

The molecular formula $C_{33}H_{44}O_{19}$ of phyllaemblicin H14 (**14**) was deduced from the HRESIMS. Its NMR spectra were similar to those of 4′-hydroxy phyllaemblicin B (**15**), except that a methine at δ_C 48.6 in **14** replaced the oxygenated quaternary carbon of C-

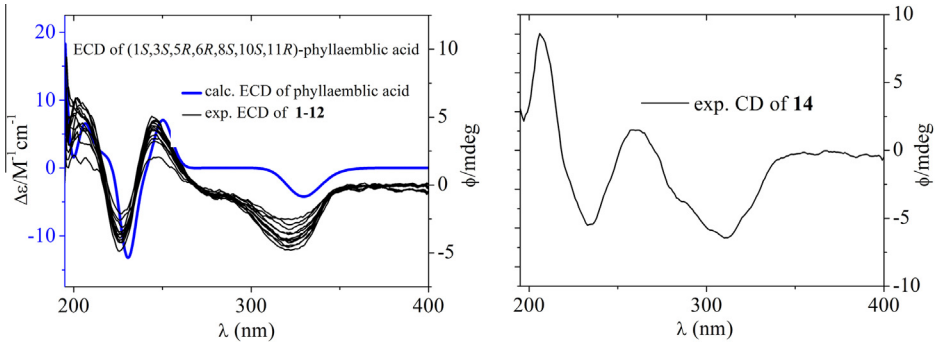

Fig. 6. Experimental ECD curves of compounds **1**–**12** and **14**, and the calculated ECD curve (TD-DFT/B3LYP-SCRF/6-311G (d,p)) of their aglycones.

Table 4
^{13}C and ^{1}H NMR Spectroscopic data for compounds **12**–**14** in CD_3OD (δ in ppm).

No.	**12**[b]		**13**[a]		**14**[a]	
	δ_C	δ_H	δ_C	δ_H	δ_C	δ_H
1	71.6, CH	3.95 brs	71.5, CH	3.94 brs	65.9, CH	4.32 brs
2	31.9, CH_2	1.81 ddd (2.7, 13.4, 15.1) 2.01 brd (15.1)	31.7, CH_2	1.80 ddd (3.1, 13.0, 14.3) 1.98[c]	35.0, CH_2	1.60 ddd (2.2, 13.0 14.5) 2.16[c]
3	32.3, CH	2.94 tt (3.2, 13.4)	32.2, CH	2.95 tt (2.4, 13.0)	31.8, CH	2.96 tt (3.2, 13.0)
4	29.9, CH_2	1.90 ddd (4.6, 13.4, 14.6) 2.45 brd (14.6)	29.6, CH_2	1.86 dd (5.3, 13.0, 15.0) 2.49 brd (15.0)	31.2, CH_2	1.86 (ddd, 4.2, 13.0, 14.5) 2.45 brd (14.5)
5	76.5, CH	4.33 brs	76.6, CH	4.31 brs	72.6, CH	4.59 brs
6	75.5, C		75.5, C		48.6, CH	2.54 t (5.7)
7	213.6, C		213.5, C		212.2, C	
8	100.6, C		100.5, C		101.0, C	
9	33.0, CH_2	2.04 dd (3.6, 14.5) 2.27 dd (3.0, 14.5)	33.0, CH_2	2.05 dd (3.2, 15.0) 2.22 dd (3.1, 15.0)	32.6, CH_2	2.00 dd (3.0, 14.7) 2.16[c]
10	70.9, CH	5.41 brd (3.3, 6.4)	71.4, CH	5.54 brs	70.6, CH	5.34 dd (3.0, 5.8)
11	34.5, CH	2.20 m	34.4, CH	2.21[c]	34.5, CH	2.16[c]
12	63.5, CH_2	3.60 m 4.05 dd (11.3, 11.3)	63.4, CH_2	3.61[c] 3.98[c]	63.8, CH_2	3.59 dd (4.8, 11.5) 4.02 dd (11.5, 11.5)
13	175.9, C		176.2, C		176.1, C	
14	13.3, CH_3	0.89 d (6.9)	13.2, CH_3	0.88 d (7.5)	13.1, CH_3	0.90 d (7.0)
1′	132.2, C		114.7, C		122.9, C	
2′	130.2, CH	8.21 d (8.2)	161.9, C		133.3, CH	8.08 d (8.0)
3′	131.0, CH	7.62 t (8.2)	119.0, CH	7.03 dd (1.0, 8.0)	116.5, CH	6.94 d (8.0)
4′	134.7, CH	7.72 t (8.2)	137.4, CH	7.59 ddd (1.8, 8.0, 8.4)	163.4, C	
5′	131.0, CH	7.62 t (8.2)	121.2, CH	7.06 ddd (1.0, 8.0, 8.4)	116.5, CH	6.94 d (8.0)
6′	130.2, CH	8.21 d (8.2)	132.4, CH	8.12 dd (1.8, 8.0)	133.3, CH	8.08 d (8.0)
7′	167.8, C		170.3, C		168.1, C	
1″	93.8, CH	5.60 d (8.0)	93.6, CH	5.58 d (8.1)	93.7, CH	5.62 d (8.0)
2″	84.0, CH	3.32[c]	84.7, CH	3.31[c]	83.3, CH	3.51 dd (8.0, 9.1)
3″	77.5, CH	3.57 dd (8.7, 8.7)	77.5, CH	3.56 dd (9.5, 9.5)	77.9, CH	3.63 dd (9.1, 9.1)
4″	70.1, CH	3.53[c]	70.1, CH	3.50 dd (9.5, 9.5)	70.6, CH	3.55 dd (9.1, 9.1)
5″	79.1, CH	3.41 ddd (2.3, 5.6, 8.5)	79.1, CH	3.40 m	79.1, CH	3.42[c]
6″	62.4, CH_2	3.78 dd (5.6, 12.3) 3.92 brd (12.3)	62.4, CH_2	3.75 dd (5.1, 12.2) 3.90 dd (2.3, 12.2)	62.3, CH_2	3.80 dd (5.8, 12.1) 3.93 dd (2.0,12.1)
1‴	104.9, CH	4.14 d (8.0)	105.2, CH	4.18 d (7.9)	106.3, CH	4.22 d (7.8)
2‴	82.4, CH	3.45 dd (8.0, 9.3)	85.4, CH	3.25 dd (7.9, 9.0)	76.0, CH	3.13 dd (7.8, 9.0)
3‴	87.0, CH	3.50 dd (9.3, 9.3)	77.8, CH	3.33[c]	77.6, CH	3.27 dd (9.0, 9.0)
4‴	69.1, CH	3.37 dd (9.3, 9.3)	70.1, CH	3.30 dd (9.5, 9.5)	70.6, CH	3.27 dd (9.0, 9.0)
5‴	76.9, CH	2.63 ddd (9.3, 2.5, 2.5)	77.1, CH	2.55 dt (9.5, 3.3)	77.6, CH	2.73 ddd (3.4, 3.5, 9.0)
6‴	62.1, CH_2	3.51[c], 3.56[c]	61.5, CH_2	3.53 m	61.7, CH_2	3.56[c], 3.61[c]
1⁗	106.1, CH	4.64 d (8.0)	107.4, CH	4.48 d (7.2)		
2⁗	73.4, CH	3.62 dd (8.0, 9.6)	73.9, CH	3.65 dd (7.2, 9.2)		
3⁗	74.5, CH	3.54 dd (3.5, 9.6)	74.2, CH	3.56 dd (3.7, 9.2)		
4⁗	69.9, CH	3.85 m	69.7, CH	3.82 brs		
5⁗	67.0, CH_2	3.63 brd (12.3) 3.98 dd (2.5, 12.3)	67.8, CH_2	3.63 dd (1.6, 12.7) 3.99[c]		
1⁗′	104.5, CH	4.62 d (8.0)				
2⁗′	75.4, CH	3.26 dd (8.0, 9.1)				
3⁗′	78.4, CH	3.39 dd (9.1, 9.1)				
4⁗′	71.6, CH	3.31 dd (9.1, 9.1)				
5⁗′	78.3, CH	3.40 m				
6⁗′	62.6, CH_2	3.66[c], 3.92[c]				

[a] Data were recorded at 150 MHz for ^{13}C or 600 MHz for ^{1}H.
[b] Data were recorded at 200 MHz for ^{13}C or 800 MHz for ^{1}H.
[c] Overlapped.

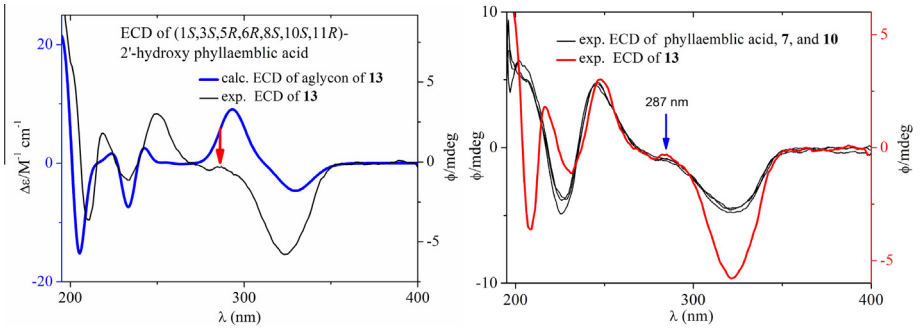

Fig. 7. Experimental ECD curves of phyllaemblic acid, compounds **7**, **10**, and **13**, and the calculated ECD curve (TD-DFT/B3LYP-SCRF/6-311G (d,p)) of the aglycone of **13**.

6 (δ_C 75.9) in **15**. This led to up-field shifts of C-1 and C-5, and a down-field shift of C-2 in **14**. The methine at δ_C 48.6 was assigned as C-6, based on the ^{1}H–^{1}H COSY correlations of its corresponding proton (δ_H 2.54, 1H, t, J = 5.7 Hz, H-6) with H-1 and H-5. The coupling constant of H-6 and its ROESY correlations with H-1 and H-5 suggested that H-6 was β-orientated. Therefore, the relative configurations of rings A and C were determined to be the same with those of **5**. Moreover, compound **14** had a similar ECD curve to that of phyllaemblic acid. Thus, the absolute configuration of **14** was established as 1*S*, 3*S*, 5*R*, 6*R*, 8*S*, 10*S*, 11*R*.

2.2. Antiviral activities

Isolated compounds (**2**–**3**, **6**–**8**, **11**–**12**, **15**–**17**) with an amount greater than 10 mg were evaluated for their antiviral activities against enterovirus 71 (EV71), influenza A virus strain H3N2, herpes simplex virus (HSV-1), and coxsackie virus B3 (CVB3) (Table 5). Compound **6** displayed inhibitory activity against HSV-1, whereas **8** and **12** showed anti CVB3 activities. The known compounds, phyllaemblicin B (**15**) and glochicoccinoside D (**17**), displayed anti-viral activities against influenza A virus strain H3N2, with IC_{50} values of 2.6 ± 0.7 and 4.5 ± 0.6 μg/ml, respectively, compared to the positive control ribavirin (IC_{50} = 25.0 ± 0.5 μg/ml). Compounds **16** and **17** also exhibited inhibitory activities against hand, foot and mouth virus EV71, with IC_{50}s of 2.6 ± 0.8 and 2.6 ± 0.7 μg/ml, respectively, whereas the positive control ribavirin gave an IC_{50} = 158.7 ± 3.3 μg/ml. Compounds **2**, **3**, **7** and **11** had no inhibitory activities towards the tested viruses with concentrations above their CC_{50} values.

2.3. Cytotoxicity activities

All isolates were evaluated for their cytotoxicities against five human cancer cell lines, i.e., lung cancer (A-549), human myeloid leukemia (HL-60), breast cancer (MCF-7), hepatocellular carcinoma (SMMC-7721), and colon cancer (SW480). Cis-platin was a broad-spectrum first-line anti-tumor drug, and was utilized as a positive control. Only phyllaemblicins H1–H2 (**1**–**2**) showed cytotoxicities (Table 6). Especially 6″-acetylated phyllaemblicin B (**2**) selectively inhibited the growth of A-549 and SMMC-7721 cell lines, with IC_{50} values of 4.7 ± 0.7 and 9.9 ± 1.3 μM, respectively. Acetylation of the saccharide moiety of norbisabolane sesquiterpenoid glycosides can thus significantly improve their cytotoxicities.

3. Conclusion

Fourteen new norbisabolane sesquiterpenoid glycosides, phyllaemblicins H1–H14, were discovered from the roots of *P. emblica*. These compounds have the rare norbisabolane sesquiterpenoid aglycone and various saccharide moieties (S_1–S_{14}). The established pre-column derivatization/chiral separation/DAD detection method takes advantages of low sample consumption (0.5–1.0 mg) and simple operation, by which the absolute configurations of the monosaccharides can be determined rapidly. Using the TDDFT calculated ECD method, the absolute configurations of the aglycones were established. Moreover, the main constituents of this plant, phyllaemblicin B (**15**) and glochicoccinoside D (**17**), showed potential anti-viral activities against H3N2 and EV71. Phyllaemblicin H1 (**1**) displayed cytotoxicity against human caner cell lines A-549 and SMMC-7721.

4. Experimental

4.1. General procedures

IR and UV spectra were measured on a Bruker Tensor 27 spectrometer with KBr pellets and Shimadzu UV 2401PC, respectively. 1D and 2D NMR spectra were run on Bruker AM-400, DRX-500 and AVANCE III-600 and AVANCE-800 NMR spectrometers operating at 400, 500 and 600 and 800 MHz for ^{1}H, and 100, 125 and 150 and 200 MHz for ^{13}C, respectively. Coupling constants are expressed in Hertz and chemical shifts are given on a ppm scale with solvents as internal standard. ESI-MS and HRESIMS were measured at Bruker HCT/Esquire and Agilent G6230. ECD and optical rotations were detected at Applied Photophysics and Jasco P-1020. The high performance liquid chromatography apparatus was an Agilent 1260 with a DAD detector. Column chromatography (CC) was performed with Sephadex LH-20 (Pharmacia Fine Chemical Co., Ltd. Uppsala, Sweden), Diaion HP20SS (Mitsubishi Chemical Co., Tokyo, Japan), MCI-gel CHP20P (Mitsubishi Chemical Co., Tokyo, Japan), RP-8 gel (40–60 μm, Merck, Darmstadt, Germany), Toyopearl HW-40C (TOSOH, Japan), Chromatorex ODS (Fuji Silysia Chemical Co. Ltd), silica gel (200–300 mesh, Qingdao Hailang Group Co., Ltd. Qingdao, People's Republic of China) and a 250 × 9.4 mm, i.d., 5 μm Sunfire C_{18} column (Waters), respectively. A CHIRALPAK AD-H column (i.d., 5 μm, 4.6 × 250 mm, Daicel corporation) was used for chiral separation. TLC was carried out on precoated silica gel GF254 plates, which were visualized by ultraviolet and spraying with 10% H_2SO_4 in EtOH solution. Quantum chemical calculations were carried out at HPC Center, Kunming Institute of Botany, CAS, China.

4.2. Plant materials

Roots of *P. emblica* were collected in Baoshan City, Yunnan Province, People's Republic of China, and identified by Prof. C. R. Yang (Kunming Institute of Botany, Chinese Academy of Sciences). A voucher specimen (KIB-ZL-0100020) is deposited in the State Key Laboratory of Phytochemistry and Plant Resource

Table 5
Anti-viral activities of the isolated compounds (IC_{50} μg/ml).[a]

Compounds	H3N2		EV71		CVB3		HSV-1	
	IC_{50}	CC_{50}	IC_{50}	CC_{50}	IC_{50}	CC_{50}	IC_{50}	CC_{50}
6	ND	ND	ND	ND	NA	26.7 ± 2.4	10.5 ± 1.1	26.7 ± 2.4
8	ND	ND	ND	ND	76.0 ± 4.8	106.8 ± 3.7	NA	106.8 ± 3.7
12	ND	ND	ND	ND	21.0 ± 1.8	55.1 ± 0.7	NA	55.1 ± 0.7
15	2.6 ± 0.7	6.9 ± 0.9	NA	6.9 ± 0.9	NA	6.9 ± 0.9	NA	6.9 ± 0.9
16	NA	13.4 ± 1.5	2.6 ± 0.8	10.0 ± 1.9	NA	13.4 ± 1.5	NA	9.0 ± 1.5
17	4.5 ± 0.6	13.4 ± 2.1	2.6 ± 0.7	9.9 ± 1.7	NA	13.4 ± 2.1	NA	13.4 ± 2.1
Ribavirin	25.0 ± 0.5	>500	158.7 ± 3.3	>500	ND	ND	ND	ND
GH	ND	ND	ND	ND	27.2 ± 0.8	>200	ND	ND
Acyclovir	ND	ND	ND	ND	ND	ND	0.033 ± 0.007	>200

NA: not active above the concentration of CC_{50}. ND: not detected. GH: Guanidine hydrochloride.
[a] Compound concentration reducing the viability of MDCK or Vero cells culture by 50%.

Table 6
Cytotoxic activities of compounds **1** and **2** (IC_{50} μM).

Compounds	A-549	HL-60	MCF-7	SMMC-7721	SW480
1	4.7 ± 0.7	18.9 ± 1.1	18.8 ± 0.7	9.9 ± 1.3	18.4 ± 0.6
2	12.3 ± 0.3	28.6 ± 1.0	>40	17.5 ± 1.0	32.9 ± 1.5
Cisplatin	3.6 ± 0.5	1.0 ± 0.2	13.0 ± 0.8	3.3 ± 0.4	16.3 ± 1.1

in West China of Kunming Institute of Botany, Chinese Academy of Sciences.

4.3. Extraction and isolation

Air dried roots of *P. emblica* (109 kg) were extracted with EtOH:H_2O (500 L, 70:30, v/v) under conditions of reflux for three times (each time 2 h) to give an extract (7.8 kg), which was suspended in H_2O (22.5 L) and partitioned with *n*-BuOH. The organic layer was concentrated in vacuo and subjected to Diaion HP20SS CC, eluted with CH_3OH:H_2O (0:100 to 100:0), to afford four major fractions (Fr.1–4). Fr.3 (400 g) was applied to a silica gel column, gradient eluted with $CHCl_3$:CH_3OH:H_2O (50:1:0 to 7:3:0.5) to give seven sub-fractions (Fr.A–Fr.G). Fr.A was subjected to Sephadex LH-20 CC, eluted with CH_3OH:H_2O (0:100 to 80:20) to afford Fr.A1–Fr.A2. Fr.A1 (3.2 g) was passed through a MCI-gel CHP20P column, eluted with CH_3OH:H_2O (30:70 to 90:10) to give four fractions (Fr.A1.1–Fr.A1.4). Fr.A1.4 was purified by Toyopearl HW-40C CC, eluted with CH_3OH:H_2O (0:100 to 30:70) to give **12** (15 mg). Fr.B was passed through Sephadex LH-20 column eluting with CH_3OH:H_2O (0:100 to 30:70), to afford Fr.B1–Fr.B2. Fr.B1 was fractionated by MCI-gel CHP20P CC, eluted with CH_3OH:H_2O (30:70 to 80:20), to afford Fr.B1.1–Fr.B1.6. Fr.B1.2 was fractionated by Toyopearl HW-40C CC, eluted with CH_3OH:H_2O (0:100 to 30:70), to give Fr.B1.2.1–1.2.2, and Fr.B1.2.1 was purified by RP-8 CC, eluted with CH_3OH:H_2O (30:70 to 80:20), to afford **11** (15 mg). Fr.B1.5 was purified by Toyopearl HW-40C CC, eluted with CH_3OH:H_2O (0:100 to 30:70) and preparative HPLC (CH_3CN:H_2O, 15:85 to 30:70), to afford **9** (2 mg). Fr.B1.6 was passed through a Toyopearl HW-40C column, eluted with CH_3OH:H_2O (0:100 to 30:70) to give Fr.B1.6.1–1.6.4, and Fr.B1.6.2 was purified by RP-8 CC, eluted with CH_3OH:H_2O (30:70 to 80:20) to afford **16** (5.0 g). Fr.B1.6.3 was applied to a RP-8 column, eluted with CH_3OH:H_2O (30:70 to 80:20), to afford **8** (24 mg) and **13** (3 mg). Fr.C was passed through a Sephadex LH-20 column, eluted with CH_3OH:H_2O (0:100 to 80:20), to afford Fr.C1–Fr.C4. Fr.C2 was applied to a RP-8 column, eluted with CH_3OH:H_2O (30:70 to 80:20) to produce Fr.C2.1–2.6. Fr.C2.5 was purified by Toyopearl HW-40C CC, eluted with CH_3OH:H_2O (0:100 to 30:70) to afford **17** (4.1 g). Fr.C2.6 was subjected to preparative HPLC (CH_3CN:H_2O, 15:85 to 30:70) to give **7** (28 mg), and **10** (6 mg). Fr.D (73 g) was passed through a Sephadex LH-20 column, eluting with CH_3OH:H_2O (0:100 to 80:20), to afford Fr.D1–D4. Fr.D2 was purified by Chromatorex ODS CC, eluted with CH_3OH:H_2O (30:70 to 80:20), to give **15** (38 g). Fr.E (24.4 g) was applied to a Sephadex LH-20 column, eluted with CH_3OH:H_2O (0:100 to 80:20), to afford Fr.E1–Fr.E3. Fr.E1 was fractionated on a RP-8 column, eluted with CH_3OH:H_2O (30:70 to 80:20), to afford Fr.E1.1–Fr.E1.8. Fr.E1.2 was applied to a Toyopearl HW-40C column, eluted with CH_3OH:H_2O (0:100 to 30:70), to give Fr.E1.2.1–1.2.3. Fr.E1.2.2 was separated using silica gel CC and preparative HPLC (CH_3CN:H_2O, 15:85 to 30:70) to afford **14** (6 mg) and **3** (10 mg). Fr.F (24.4 g) was passed over a Sephadex LH-20 column, eluted with CH_3OH:H_2O (0:100 to 80:20), to afford Fr.F1–Fr.F3. Fr.F1 was fractionated by RP-8 CC, eluted with CH_3OH:H_2O (30:70 to 80:20), to produce Fr.F1.1–1.9. Fr.F1.2 was subjected to silica gel CC to afford Fr.F1.2.1–1.2.4, and Fr.F1.2.2 was purified by preparative HPLC, eluted with CH_3CN:H_2O (15:85 to 30:70), to yield **5** (3 mg). Fr.F1.3 was passed through a Toyopearl HW-40C column, eluted with CH_3OH:H_2O (0:100 to 30:70), to give Fr.F1.3.1–1.3.5. Fr.F1.3.2 was purified by preparative HPLC, eluted with CH_3CN:H_2O (15:85 to 30:70), to yield **2** (17 mg). Fr.F1.3.4 was subjected to preparative HPLC, eluted with CH_3CN:H_2O (15:85 to 30:70), to afford **1** (3 mg), **4** (2 mg) and **6** (21 mg).

4.3.1. Phyllaemblicin H1 (*1*)

White amorphous powder; $[\alpha]_D^{25}$ = +6.4 (*c* 0.8, CH_3OH); UV (MeOH) λ_{max} (log ε) 200.6 (1.10), 228 (1.11), 272 (0.15) nm; ECD (in MeOH, λ_{max} [nm], ϕ[mdeg]) 205 (3.9), 227 (−4.3), 245 (3.4), 322 (−4.3); IR (KBr) ν_{max} 3431, 2925, 1719, 1280, 1078 cm^{-1}; For ^1H NMR (CD_3OD, 600 MHz) and ^{13}C NMR (CD_3OD, 150 MHz) spectroscopic data, Table 1; MS (ESI): *m/z* 821 $[M+Cl]^-$; HRMS (ESI): *m/z* 831.2556 $[M+HCOO]^-$ (calcd for $C_{36}H_{47}O_{22}$, 831.2565).

4.3.2. Phyllaemblicin H2 (*2*)

White amorphous powder; $[\alpha]_D^{25}$ = +4.7 (*c* 1.2, CH_3OH); UV (MeOH) λ_{max} (log ε) 200.6 (1.08), 228 (1.08), 272 (0.19) nm; ECD (in MeOH, λ_{max} [nm], ϕ[mdeg]) 204 (5.2), 226 (−4.0), 246 (4.2), 322 (−4.7); IR (KBr) ν_{max} 3431, 2925, 1719, 1280, 1078 cm^{-1}; For ^1H NMR (CD_3OD, 600 MHz) and ^{13}C NMR (CD_3OD, 150 MHz) spectroscopic data, see Table 1; MS (ESI): *m/z* 821 $[M+Cl]^-$; HRMS (ESI): *m/z* 831.2556 $[M+HCOO]^-$ (calcd for $C_{36}H_{47}O_{22}$, 831.2565).

4.3.3. Phyllaemblicin H3 (*3*)

White amorphous powder; $[\alpha]_D^{25}$ = +10.4 (*c* 1.2, CH_3OH); UV (MeOH) λ_{max} (log ε) 200.0 (1.06), 228.6 (1.05) nm; ECD (in MeOH, λ_{max} [nm], ϕ[mdeg]) 205 (5.2), 226 (−4.6), 246 (3.8), 321 (−4.5); IR (KBr) ν_{max} 3431, 2925, 1719, 1280, 1078 cm^{-1}; For ^1H NMR (CD_3OD, 600 MHz) and ^{13}C NMR (CD_3OD, 150 MHz) spectroscopic

data, see Table 1; MS (ESI): *m/z* 749 $[M+Cl]^-$; HRMS (ESI): *m/z* 759.2335 $[M+HCOO]^-$ (calcd for $C_{33}H_{43}O_{20}$, 759.2353).

*4.3.4. Phyllaemblicin H4 (**4**)*

White amorphous powder; $[\alpha]_D^{25}$ = +2.4 (*c* 0.6, CH_3OH); UV (MeOH) λ_{max} (log ε) 200.2 (1.13), 228.4 (1.13), 272.6 (0.18) nm; ECD (in MeOH, λ_{max} [nm], ϕ[mdeg]) 208 (2.2), 226 (−3.9), 246 (3.0), 321 (−4.0); IR (KBr) ν_{max} 3424, 2928, 1719, 1280, 1080 cm^{-1}; For ^1H NMR (CD_3OD, 600 MHz) and ^{13}C NMR (CD_3OD, 150 MHz) spectroscopic data, see Table 1; MS (ESI): *m/z* 737 $[M+Cl]^-$; HRMS (ESI): *m/z* 759.2346 $[M+HCOO]^-$ (calcd for $C_{33}H_{43}O_{20}$, 759.2353).

*4.3.5. Phyllaemblicin H5 (**5**)*

White amorphous powder; $[\alpha]_D^{25}$ = +13.2 (*c* 0.9, CH_3OH); UV (MeOH) λ_{max} (log ε) 200.0 (1.05), 228.2 (1.02), 272.4 (0.03) nm; ECD (in MeOH, λ_{max} [nm], ϕ[mdeg]) 202 (5.7), 226 (−4.4), 245 (4.3), 323 (−4.9); IR (KBr) ν_{max} 3425, 2930, 1719, 1280, 1076 cm^{-1}; For ^1H NMR (CD_3OD, 800 MHz) and ^{13}C NMR (CD_3OD, 100 MHz) spectroscopic data, see Table 2; MS (ESI): *m/z* 751 $[M+Na]^+$; HRMS (ESI): *m/z* 773.2486 $[M+HCOO]^-$ (calcd for $C_{34}H_{45}O_{20}$, 773.2510).

*4.3.6. Phyllaemblicin H6 (**6**)*

White amorphous powder; $[\alpha]_D^{25}$ = +42.3 (*c* 0.9, CH_3OH); UV (MeOH) λ_{max} (log ε) 200.4 (1.13), 228.6 (1.15), 272.8 (0.22) nm; ECD (in MeOH, λ_{max} [nm], ϕ[mdeg]) 204 (5.4), 228 (−3.4), 244 (5.0), 321 (−4.9); IR (KBr) ν_{max} 3429, 2927, 1716, 1280, 1114 cm^{-1}; For ^1H NMR (CD_3OD, 600 MHz) and ^{13}C NMR (CD_3OD, 150 MHz) spectroscopic data, Table 2; MS (ESI): *m/z* 605 $[M+Na]^+$; HRMS (ESI): *m/z* 627.1926 $[M+HCOO]^-$ (calcd for $C_{28}H_{35}O_{16}$, 627.1931).

*4.3.7. Phyllaemblicin H7 (**7**)*

White amorphous powder; $[\alpha]_D^{25}$ = +33.5 (*c* 1.1, CH_3OH); UV (MeOH) λ_{max} (log ε) 199.8 (1.09), 228.8 (1.11), 271.4 (0.11) nm; ECD (in MeOH, λ_{max} [nm], ϕ[mdeg]) 206 (4.4), 227 (−5.6), 245 (4.6), 321 (−5.4); IR (KBr) ν_{max} 3429, 2929, 1718, 1280, 1075 cm^{-1}; For ^1H NMR (CD_3OD, 800 MHz) and ^{13}C NMR (CD_3OD, 100 MHz) spectroscopic data, see Table 2; MS (ESI): *m/z* 767 $[M+Na]^+$; HRMS (ESI): *m/z* 789.2440 $[M+HCOO]^-$ (calcd for $C_{34}H_{45}O_{21}$, 789.2459).

*4.3.8. Phyllaemblicin H8 (**8**)*

White amorphous powder; $[\alpha]_D^{25}$ = +35.0 (*c* 0.8, CH_3OH); UV (MeOH) λ_{max} (log ε) 200.0 (1.13), 229.0 (1.10), 271.8 (0.05) nm; ECD (in MeOH, λ_{max} [nm], ϕ[mdeg]) 201 (4.9), 227 (−4.5), 246 (3.9), 322 (−4.7); IR (KBr) ν_{max} 3430, 2926, 1717, 1281, 1076 cm^{-1}; For ^1H NMR (CD_3OD, 800 MHz) and ^{13}C NMR (CD_3OD, 125 MHz) spectroscopic data, see Table 3; MS (ESI): *m/z* 911 $[M+Cl]^-$; HRMS (ESI): *m/z* 875.2814 $[M-H]^-$ (calcd for $C_{38}H_{51}O_{23}$, 875.2827).

*4.3.9. Phyllaemblicin H9 (**9**)*

White amorphous powder; $[\alpha]_D^{25}$ = −0.6 (*c* 0.4, CH_3OH); UV (MeOH) λ_{max} (log ε) 200.6 (0.93), 228.6 (0.94) nm; ECD (in MeOH, λ_{max} [nm], ϕ[mdeg]) 207 (3.7), 226 (−3.7), 245 (4.3), 322 (−4.2); For ^1H NMR (CD_3OD, 600 MHz) and ^{13}C NMR (CD_3OD, 150 MHz) spectroscopic data, see Table 3; MS (ESI): *m/z* 751 $[M+Na]^+$; HRMS (ESI): *m/z* 743.2391 $[M-H]^-$ (calcd for $C_{33}H_{43}O_{19}$, 743.2404).

*4.3.10. Phyllaemblicin H10 (**10**)*

White amorphous powder; $[\alpha]_D^{25}$ = −7.3 (*c* 0.6, CH_3OH); UV (MeOH) λ_{max} (log ε) 200.0 (1.01), 228.6 (1.07), 272.2 (0.06) nm; ECD (in MeOH, λ_{max} [nm], ϕ[mdeg]) 203 (5.9), 227 (−4.1), 246 (4.7), 322 (−5.1); IR (KBr) ν_{max} 3424, 2926, 1717, 1605, 1280, 1077, 1040 cm^{-1}; For ^1H NMR (CD_3OD, 500 MHz) and ^{13}C NMR (CD_3OD, 125 MHz) spectroscopic data, see Table 3; MS (ESI): *m/z* 911 $[M+Cl]^-$; HRMS (ESI): *m/z* 921.2867 $[M+HCOO]^-$ (calcd for $C_{39}H_{53}O_{25}$, 921.2881).

*4.3.11. Phyllaemblicin H11 (**11**)*

White amorphous powder; $[\alpha]_D^{25}$ = −7.9 (*c* 0.3, CH_3OH); UV (MeOH) λ_{max} (log ε) 201.4 (1.28), 227.2 (1.06), 274.0 (0.49) nm; ECD (in MeOH, λ_{max} [nm], ϕ[mdeg]) 207 (1.4), 227 (−2.6), 247 (2.1), 322 (−3.2); For ^1H NMR (CD_3OD, 800 MHz) and ^{13}C NMR (CD_3OD, 150 MHz) spectroscopic data, see Table 3; MS (ESI): *m/z* 767 $[M+Na]^+$; HRMS (ESI): *m/z* 743.2384 $[M-H]^-$ (calcd for $C_{33}H_{43}O_{19}$, 743.2404).

*4.3.12. Phyllaemblicin H12 (**12**)*

White amorphous powder; $[\alpha]_D^{25}$ = +7.1 (*c* 1.6, CH_3OH); UV (MeOH) λ_{max} (log ε) 201.8 (1.24), 228.2 (1.12) nm; ECD (in MeOH, λ_{max} [nm], ϕ[mdeg]) 208 (3.2), 228 (−2.5), 245 (3.4), 322 (−3.6); IR (KBr) ν_{max} 3424, 2928, 1711, 1283, 1078 cm^{-1}; For ^1H NMR (CD3OD, 800 MHz) and ^{13}C NMR (CD_3OD, 200 MHz) spectroscopic data, see Table 4; MS (ESI): *m/z* 1073 $[M+Cl]^-$; HRMS (ESI): *m/z* 1037.3338 $[M-H]^-$ (calcd for $C_{44}H_{61}O_{28}$, 1037.3355).

*4.3.13. Phyllaemblicin H13 (**13**)*

White amorphous powder; $[\alpha]_D^{25}$ = −31.9 (*c* 1.1, CH_3OH); UV (MeOH) λ_{max} (log ε) 206.0 (1.39), 235.8 (0.96), 306.4 (0.55) nm; ECD (in MeOH, λ_{max} [nm], ϕ[mdeg]) 211 (−3.6), 220 (1.6), 233 (−1.4), 249 (2.7), 289 (−1.1), 324 (−6.5); IR (KBr) ν_{max} 3419, 2927, 1717, 1615, 1081 cm^{-1}; For ^1H NMR (CD_3OD, 600 MHz) and ^{13}C NMR (CD_3OD, 150 MHz) spectroscopic data, see Table 4; MS (ESI): *m/z* 891 $[M-H]^-$; HRMS (ESI): *m/z* 891.2765 $[M-H]^-$ (calcd for $C_{38}H_{51}O_{24}$, 891.2776).

*4.3.14. Phyllaemblicin H14 (**14**)*

White amorphous powder; $[\alpha]_D^{25}$ = −9.4 (*c* 1.0, CH_3OH); UV (MeOH) λ_{max} (log ε) 201.8 (1.24), 257.8 (1.12) nm; ECD (in MeOH, λ_{max} [nm], ϕ[mdeg]) 207 (8.1), 235 (−5.5), 261 (1.4), 310 (−7.0); IR (KBr) ν_{max} 3428, 2928, 1708, 1609,1280, 1078 cm^{-1}; For ^1H NMR (CD_3OD, 600 MHz) and ^{13}C NMR (CD_3OD, 150 MHz) spectroscopic data, see Table 4; MS (ESI): *m/z* 767 $[M+Na]^+$; HRMS (ESI): *m/z* 743.2401 $[M-H]^-$ (calcd for $C_{33}H_{43}O_{19}$, 743.2404).

*4.4. Acid hydrolysis of compounds **3**–**5**, **7**, and **10***

Compounds **3**–**5**, **7** and **10** (each 0.5–1.0 mg) were dissolved in 2 M HCl (400 μL) in a vial separately. Then, each vial was sealed and incubated at 80 °C in a water bath. After 6 h, each solution was cooled to room temperature, and extracted with $CHCl_3$ (400 μL × 2). Each aqueous layer was neutralized by passaging over a small column with Amberlite IRA-401. TLC was used to identify the type of monosaccharide by comparing with the authentic sugars, with elution system $CHCl_3$:*n*-BuOH:MeOH:HAc:H_2O (17:10:6:2:3), and the *Rf*s of standard sugars were 0.40 for arabinose, 0.53 for 6-deoxy *β*-glucose, 0.46 for xylose and 0.35 for glucose.

4.5. Precolumn derivatization and chiral separation

The mixture of monosaccharides from compounds **3**–**5**, **7** and **10** were added separately into a small sample tube. Derivatization was carried out as reported by Honda et al. (1989). Briefly, 1-phenyl-3-methyl-5-pyrazolone (PMP) dissolved in MeOH (0.5 M, 50 μL) and NaOH solution (0.3 M, 50 μL) were added in each tube, respectively. The tubes were sealed and incubated at 70 °C for 30 min. After cooling to room temperature, HCl solution (0.1 M, 50 μL) was added, and the solution was

evaporated to dryness. The residue was partitioned between H_2O (200 μL) and $CHCl_3$ (200 μL), and the aqueous layer was evaporated to dryness. The resultant PMP-monosaccharide was dissolved in EtOH/*n*-hexane solution (1:4, v/v) and analyzed by HPLC using CHRIALPAK AD-H column, with an elution solvent system of *n*-hexane/i-PrOH (87:13) at 25 °C, and detected by DAD detector. The standard sugars were analyzed using the same methods. The retention time of standard sugars were D-glucose (15.0 min), L-glucose (17.5 min), D-xylose (15.5 min), L-xylose (16.8 min), L-arabinose (11.3 min), and D-arabinose (18.5 min), respectively.

4.6. Quantum chemical calculations

Conformational analyses were carried out using Monte Carlo search with molecular mechanics MMFF in Spartan'06 (Wavefunction Inc. Irvine, CA). The resultant conformers were re-optimized using DFT at the B3LYP-SCRF/6-311G (d, p) level using the integral equation formalism variant of the polarizable continuum model (IEF-PCM). The free energies and vibrational frequencies were calculated at the same level to confirm their stability, and no imaginary frequencies were found. The optimized low energy conformers with energy <2 kcal/mol were considered for ECD calculation. The TDDFT/B3LYP-SCRF/6-311G (d,p) method was applied to calculate the excited energies, oscillator strength and rotational strength. All the calculations were run with Gaussian '09 (Frisch et al., 2009). The excited energies and rotational strength values were used to simulate ECD spectra of each conformer by introducing the Gaussian Function. The final ECD spectra of each compound were obtained by averaging all the simulated ECD spectra of all conformers according to their excited energies and Boltzmann distribution (Lv et al., 2014a,b). The band shape of the calculated ECD curves were all 0.3 eV if there is no illustration.

4.7. Antiviral bioassay

4.7.1. Virus and cell culture

Dog kidney cells MDCK, were used as target cells for H3N2 virus infection, which were cultured in M199 (Sigma, St. Louis, USA) supplemented with 10% fetal bovine serum (FBS), 500 unit/ml ampicillin, 300 μg/ml streptomycin and 0.25 μg/ml amphotericin B. Maintenance medium (MM) was the same as M199 but containing 5% fetal bovine serum. Vero cells were used as target cells for CVB3, EV71, H3N2, HSV-1 and virus infection, which were cultured in MEM. Cell culture was maintained at 37 °C in a humidified 5% CO_2 atmosphere. Virus strains CVB3, EV71, H3N2, and HSV-1 were provided by Shanghai Municipal Center for Disease Control and Prevention. The viral titer was tested by the cytopathic end-point assay (Schmidtke et al., 2001) and expressed as 50% tissue culture infective dose (TCID50).

4.7.2. Cytotoxicity assay

MDCK, Vero cells were plated in 96-well plates in 100 μL medium, which were incubated for 24 h (5% CO_2, 37 °C) to form cell monolayers, and the test samples were added at varied concentrations. After 72 h incubation, MTT [[3-(4,5-dimethylthiazol-2-yl)-2,5-diphenyl tetrazolium bromide] solution [0.5 mg/ml in phosphate buffered saline (PBS)] was added (20 μL per well), and the incubation continued for another 4 h to give a formazan product. In each well, DMSO (200 μL) was added after the medium was removed, and it was then incubated overnight for the formazan product to dissolve completely. The absorbance of the solution was measured at 490 nm using a Bio-Rad 680. Compound concentrations reducing the viability of cells culture by 50% (CC_{50}) were calculated by regression analysis of the dose–response curves.

4.7.3. Anti-virus assay

MDCK and Vero cells were plated in 96-well plates and incubated for 24 h (5% CO_2, 37 °C) to form monolayers. Virus suspensions were added to each well and to allow the adsorption for 2 h. Then the viruses were removed and a serial twofold dilution of the tested compounds at dose below CC_{50} (50 μL per well) each with equal volume were added, and followed incubation for 72 h. The virus-induced CPE of the tests was expressed as a percentage in comparison with the parallel virus control and cell control. IC_{50} values (the concentration of test compounds required to reduce 50% of CPE) were calculated by regression analysis of the dose–response curves, and the therapeutic index (TI) was calculated from the ratio CC_{50}/IC_{50}. Ribavirin was tested as the positive control for anti EV71 and H3N2, and Guanidine hydrochloride and Acyclovir were tested as the positive control for anti CVB3 and HSV-1, respectively.

4.8. Human cancer cell cytotoxicity assay

As previously reported (Lv et al., 2013).

Acknowledgment

The authors are grateful to the members of the analytical group at State Key Laboratory of Phytochemistry and Plant Resources in West China, Kunming Institute of Botany, Chinese Academy of Sciences, for measuring the spectroscopic data. We also thank Fudan University for antiviral assay. This work was supported by the National Natural Science Foundation of China (NSFC 81473121), the 973 Program of Ministry of Science and Technology of P.R. China (2011CB915503), the National Science & Technology Support Program of China (2013BAI11B02), the 12th 5-Year National Science & Technology Supporting Program of China (2012BAI29B06), the Fourteenth Candidates of the Young Academic Leaders of Yunnan Province (Min Xu, 2011CI044) and by West Light Foundation of the Chinese Academy of Sciences.

Appendix A. Supplementary data

Supplementary data associated with this article can be found. The data include ^1H and ^{13}C NMR, HSQC, HMBC, HSQC-TOCSY, ^1H–^1H COSY, ROESY, HRESIMS spectra for compounds **1**–**14**, low energy conformers of calculated ECD, and chromatograms of standard sugars in chiral separation. These data are available free of charge via internet http://www.sciencedirect.com. Supplementary data associated with this article can be found, in the online version, at http://dx.doi.org/10.1016/j.phytochem.2015.06.001.

References

Frisch, M.J., Trucks, G.W., Schlegel, H.B., Scuseria, G.E., Robb, M.A., Cheeseman, J.R., Scalmani, G., Barone, V., Mennucci, B., Petersson, G.A., Nakatsuji, H., Caricato, M., Li, X., Hratchian, H.P., Izmaylov, A. F., Bloino, J., Zheng, G., Sonnenberg, J..L., Hada, M., Ehara, M., Toyota, K., Fukuda, R., Hasegawa, J., Ishida, M., Nakajima, T., Honda, Y., Kitao, O., Nakai, H., Vreven, T., Montgomery, J.A., Peralta, J.E., Ogliaro, F., Bearpark, M., Heyd, J.J., Brothers, E., Kudin, K.N., Staroverov, V.N., Kobayashi, R., Normand, J., Raghavachari, K., Rendell, A., Burant, J.C., Iyengar, S.S., Tomasi, J., Cossi, M., Rega, N., Millam, J.M., Klene, M., Knox, J.E., Cross, J.B., Bakken, V., Adamo, C., Jaramillo, J., Gomperts, R., Stratmann, R.E., Yazyev, O., Austin, A.J., Cammi, R., Pomelli, C., Ochterski, J.W., Martin, R.L., Morokuma, K., Zakrzewsk, V.G., Voth, G.A., Salvador, P., Dannenberg, J.J., Dapprich, S., Daniels, A.D., Farkas, O., Foresman, J.B., Ortiz, J.V., Cioslowski, J., Fox, D.J., Gaussian 09, Revision A.02, Gaussian Inc, Wallingford, CT, 2009.

Honda, S., Akao, E., Suzuki, S., Okuda, M., Kakehi, K., Nakamura, J., 1989. High performance liquid-chromatography of reducing carbonhydrates as strongly ultraviolet-absorbing and electrochemically sensitive 1-phenyl-3-methyl-5-pyrazolone derivatives. J. Anal. Biochem. 180, 351–357.

Kupchan, S.M., LaVoie, E.J., Branfman, A.R., Fei, B.Y., Bright, W.M., Bryan, R.F., 1977. Tumor inhibitors. 120. Phyllanthocin, a novel bisabolane aglycone from antileukemic glycoside, phyllanthoside. J. Am. Chem. Soc. 99, 3199–3201.

Liu, Q., Wang, Y.F., Chen, R.J., Zhang, M.Y., Wang, Y.F., Yang, C.R., Zhang, Y.J., 2009. Anti-coxsackie virus B3 norsesquiterpenoids from the roots of *Phyllanthus emblica*. J. Nat. Prod. 72, 969–972.

Lv, J.J., Xu, M., Wang, D., Zhu, H.T., Yang, C.R., Wang, Y.F., Li, Y., Zhang, Y.J., 2013. Cytotoxic bisbenzylisoquinoline alkaloids from *Stephania epigaea*. J. Nat. Prod. 76, 926–932.

Lv, J.J., Wang, Y.F., Zhang, J.M., Yu, S., Wang, D., Zhu, H.T., Cheng, R.R., Yang, C.R., Xu, M., Zhang, Y.J., 2014a. Anti-hepatitis B virus activities and absolute configurations of sesquiterpenoid glycosides from *Phyllanthus emblica*. Org. Biomol. Chem. 12, 8764–8774.

Lv, J.J., Yu, S., Wang, Y.F., Wang, D., Zhu, H.T., Cheng, R.R., Yang, C.R., Xu, M., Zhang, Y.J., 2014b. Anti-hepatitis B virus norbisabolane sesquiterpenoids from *Phyllanthus acidus* and the establishment of their absolute configurations using theoretical calculations. J. Org. Chem. 79, 5432–5447.

Moore, D.J., Powis, G., 1986. Disposition and metabolism of the antitumor glycoside phyllanthoside in mouse and beagle dog. Cancer Chemother. Pharm. 16, 218–222.

Schmidtke, M., Schnittler, U., Jahn, B., Dahse, H.M., Stelzner, A., 2001. A rapid assay for evaluation of antiviral activity against coxsackie virus B3, influenza virus A, and herpes simplex virus type 1. J. Virol. Methods 95, 133–143.

Smith, A.B., Hale, K.J., Vaccaro, H.A., 1991. Phyllanthoside phyllanthostatin synthetic studies 7. Total synthesis of dextro phyllanthocin and dextro phyllanthocindiol. J. Am. Chem. Soc. 113, 2071–2092.

Vongvanich, N., Kittakoop, P., Kramyu, J., Tanticharoen, M., Thebtaranonth, Y., 2000. Phyllanthusols A and B, cytotoxic norbisabolane glycosides from *Phyllanthus acidus* skeels. J. Org. Chem. 65, 5420–5423.

Xiao, H.T., He, H.P., Peng, J., Wang, Y.H., Yang, X.W., Hu, X.J., Hao, X.Y., Hao, X.J., 2007. Two new norbisabolane sesquiterpenoid glycosides from *Glochidion coccineum*. J. Asian Nat. Prod. Res. 10, 1–5.

Xie, Z.W., 1996. China's Medicinal Herbs. People's Health Publishing House, Beijing.

Zhang, Y.J., Tanaka, T., Iwamoto, Y., Yang, C.R., Kouno, I., 2000a. Novel norsesquiterpenoids from the roots of *Phyllanthus emblica*. J. Nat. Prod. 63, 1507–1510.

Zhang, Y.J., Tanaka, T., Iwamoto, Y., Yang, C.R., Kouno, I., 2000b. Phyllaemblic acid, a novel highly oxygenated norbisabolane from the roots of *Phyllanthus emblica*. Tetrahedron Lett. 41, 1781–1784.

Zhang, Y.J., Tanaka, T., Iwamoto, Y., Yang, C.R., Kouno, I., 2001. Novel sesquiterpenoids from the roots of *Phyllanthus emblica*. J. Nat. Prod. 64, 870–873.